Transmission length of pretensioned concrete systems – comparison of codes and test data

Article *in* Magazine of Concrete Research · May 2018
DOI: 10.1680/jmacr.17.00553

3 authors, including:

Prabha Mohandoss
Indian Institute of Technology Madras
13 PUBLICATIONS **11** CITATIONS
SEE PROFILE

Radhakrishna Pillai
Indian Institute of Technology Madras
72 PUBLICATIONS **213** CITATIONS
SEE PROFILE

Cite this article
Mohandoss P, Pillai RG and Sengupta AK
Transmission length of pretensioned concrete systems – comparison of codes and test data.
Magazine of Concrete Research,
https://doi.org/10.1680/jmacr.17.00553

Research Article
Paper 1700553
Received 15/12/2017; Revised 20/04/2018;
Accepted 27/04/2018

Keywords: compressive strength/
prestressed concrete/shear

Magazine of Concrete Research

ice publishing

Transmission length of pretensioned concrete systems – comparison of codes and test data

Prabha Mohandoss
Graduate Student, Department of Civil Engineering, Indian Institute of Technology Madras, Chennai, India

Radhakrishna G. Pillai
Associate Professor, Department of Civil Engineering, Indian Institute of Technology Madras, Chennai, India (corresponding author: pillai@iitm.ac.in)

Amlan K. Sengupta
Professor, Department of Civil Engineering, Indian Institute of Technology Madras, Chennai, India

This paper presents a comparative study of the transmission length (L_t) of pretensioned concrete (PTC) members obtained using experiments and AASHTO, ACI, BIS, Eurocode 2 and fib Model Code (fib-MC) codes. Tests on six PTC specimens (with 12·7 mm dia. strands (d_s) and effective prestress (f_{pe}) of 1214 MPa) indicated that L_t can reduce by about 20% when the concrete strength (f_{ci}) increases from about 23 to 36 MPa. A case study of the influence of L_t on the shear resistance of a typical precast hollow-core slab showed that the ACI and fib-MC codes provide conservative shear designs, whereas the IS code considers only d_s and provides a less conservative design. This paper proposes a revised tentative formula of L_t (as a function of d_s, f_{pe} and f_{ci}) to be incorporated in the IS 1343 and other codes. It is anticipated that this will lead to more rational and conservative shear designs.

Notation

A_{ps}	sum of cross-sectional areas of seven wires in a strand (mm^2)
b_w	width of the cross-section at the centroid (mm)
d	effective depth of the member (mm)
d_s	diameter of prestressing strand (mm)
f_{bpt}	bond stress at the time of releasing (MPa)
f_{ci}	compressive strength of concrete at release (MPa)
f_{ck}	characteristic compressive strength of concrete (MPa)
f_{cp}	concrete stress due to effective prestress at centroid (MPa)
f_{ctd}	design tensile strength of concrete (MPa)
f_{pe}	effective stress in prestressing steel after allowance for all prestress losses (MPa)
f_{pi}	initial prestress of strand before losses (MPa)
f_{pu}	ultimate tensile stress in strand (MPa)
f_t	maximum principal tensile stress (MPa)
f'_c	specified compressive strength of concrete (MPa)
I	moment of inertia of gross cross-section (mm^4)
k_1	factor to account for the distance of section considered from L_t
L_b	bond length (mm)
L_d	development length (mm)
L_t	transmission length (mm)
$L_{t,avg}$	average value of L_t (mm)
$L_{t,code}$	calculated value of L_t using codes (mm)
$L_{t,measured}$	experimentally measured value of L_t (mm)
$L_{t,0}$	value of L_t measured at 0 d (mm)
$L_{t,150}$	value of L_t measured at 150 d (mm)
$L_{t,200}$	value of L_t measured at 200 d (mm)
$L_{t,250}$	value of L_t measured at 250 d (mm)
Q	moment of area (mm^2)
V_c	shear capacity contributed by the concrete (kN)
V_{ci}	flexural capacity of the member (kN)
V_{cw}	web shear capacity of the member (kN)
V_n	nominal shear resistance of concrete (kN)
$V_{n,max}$	shear force (kN)
V_p	vertical component of the effective prestress (kN)
V_s	shear capacity contributed by stirrups (kN)
x	distance from the end of the member
α	correction factor for compressive strength of concrete at prestress release
α_1	factor to account for the releasing method
α_2	factor to account for the type of strand in Eurocode 2 (BSI, 2004); factor to account for the action effect in fib-MC (fib, 2010)
α_3	factor to account for pretensioned strand in fib-MC (fib, 2010)
ε_c	strain on the concrete surface
$\varepsilon_{c,max}$	maximum strain on the concrete surface
ε_{ce}	effective strain on the concrete surface
$\varepsilon_{c(x)}$	strain on the concrete surface at distance x
$\varepsilon'_{c(x)}$	smoothed strain on the concrete surface at distance x
ε_{pe}	effective strain in the strand
ε_{pi}	strain in the strand due to initial prestress before losses
$\varepsilon_{ps(x)}$	strain in the strand at distance x after transfer
η_{p1}	factor to account for the type of tendon in fib-MC (fib, 2010)
η_{p2}	factor to account for the position of the tendon in fib-MC (fib, 2010)
λ	factor to account for the concrete type

Introduction

Pretensioned concrete (PTC) systems with seven-wire strand are widely used as girders in bridges or buildings and in hollow-core slabs (HSCs) in buildings. In PTC elements, the prestress from the strand is transferred to the surrounding concrete through the bond between the strand and the concrete (termed as 'S–C bond' herein). If the prestress is not adequately transferred within a particular distance from the free ends of the strands, the shear-critical sections, near the support, might not have the required prestress to resist shear stresses. Inadequate transmission length could result in shear cracks under external loading (Elliott, 2014). The transmission length L_t is defined as the length of a strand required to develop an effective prestress (f_{pe}). Figure 1 shows an example of the shear failure of a pretensioned HCS, which is widely used in buildings. Such shear cracks can occur as the result of (*i*) low-strength concrete, (*ii*) poor construction practices, (*iii*) low bond strength or (*iv*) inadequate design provisions for transmission length, L_t.

Figure 2(a) shows the idealised bilinear curve, exhibiting the development of stress in the strand along the distance x from the end of the member. As shown by Line 1, the stress is zero at the end of the member (at $x = 0$) and gradually increases to f_{pe} at the end of the transmission zone (at $x = L_t$). Further, as depicted by Line 2, under ultimate loading conditions, the stress along the strand increases linearly from f_{pe} (at $x = L_t$) to the ultimate stress (f_{pu}) (at $x = L_d$). The length required to increase the stress in the strand from f_{pe} to f_{pu} is defined as the bond length (L_b), which is the difference between L_d and L_t. Figure 2(b) shows the strain in the strand (ε_{ps}) and the strain on the concrete surface (ε_c) at the time of prestress transfer; ε_{pe} and ε_{ce} are the effective strains (after the initial losses) in the strand and on the concrete surface, respectively. The sum of ε_{pe} and ε_{ce} is equal to ε_{pi}, which is the strain in the strand due to the initial prestress.

The shear demand is high in the transmission zone (e.g. near support regions) of PTC systems. Underestimation of L_t can lead to less conservative shear designs. Therefore, a realistic estimation of L_t is important for achieving adequate shear capacity. This paper discusses the existing formulations for estimating L_t, their limitations and experimental observations on the influence of compressive strength of concrete on L_t and time-dependent increase in L_t. Also, the influence of L_t on the shear capacity of HCS is presented as a case study.

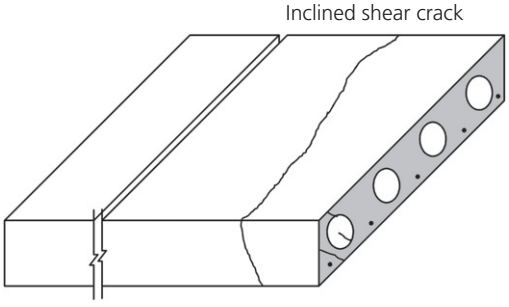

Figure 1. Shear crack in pretensioned slab unit

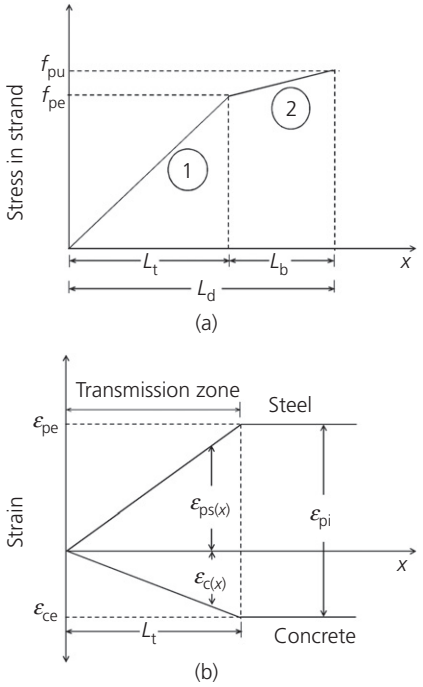

Figure 2. (a) Idealised stress development in the strand; (b) strain development in the steel and concrete at the transfer of prestress

Mechanisms of S–C bond

Figure 3 shows the adhesion, friction and mechanical interlock mechanisms that can contribute to the S–C bond in PTC systems (Hanson and Kaar, 1959; Janney, 1954). Adhesion plays a minimal role in transferring the prestress because the slip of strand with respect to the concrete during the transfer of prestress can destroy the adhesive bond formed during early hardening of the concrete (Barnes *et al.*, 2003). Friction and mechanical interlock have significant roles in transferring the prestress and developing the S–C bond. Friction in the transmission zone is mainly contributed by the Hoyer effect, which is explained as follows. At the time of prestress transfer or release, the strand can undergo longitudinal shortening. This can result in a corresponding increase in the lateral dimensions of the strand, owing to the Poisson effect. This phenomenon is known

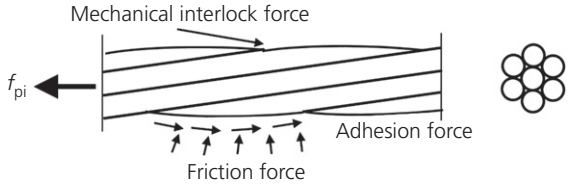

Figure 3. Mechanisms of S–C bond in a PTC system

as the Hoyer effect (Hoyer and Friedrich, 1939). This expansion induces compressive stresses perpendicular to the S–C interface, resulting in an increased frictional force, which in turn enhances the bond. In addition, the mechanical interlock (due to the helical outer wires of the strands) provides the bearing stress, which also contributes to bond stress development.

Factors affecting L_t

The compressive strength of concrete at the time of prestress transfer (f_{ci}), the diameter of the strand (d_s), the texture and surface condition of the strand, confinement due to the presence of stirrups, the method of prestress transfer (gradual or sudden), and other time-dependent effects (creep and shrinkage) can affect the transmission length in a PTC member. The following is a discussion of these factors.

Compressive strength of concrete at prestress transfer (f_{ci})

In practice, the prestress is transferred when the concrete attains about 60% of its target characteristic compressive strength (f_{ck}). As the concrete gains strength, the stiffness increases, which in turn increases the frictional stress (Barnes *et al.*, 2003). This results in a shorter L_t, owing to an improved bond (Oh and Kim, 2000). Several empirical equations and analytical models are available to determine L_t as a function of f_{ci} and other parameters, as shown in Figure 4 and discussed later (Barnes *et al.*, 2003; Cousins *et al.*, 1990; Lane, 1998; Mahmoud *et al.*, 1999; Martí-Vargas *et al.*, 2012a; Mitchell *et al.*, 1993; Ramirez-Garcia *et al.*, 2016; Zia and Mostafa, 1977). The compressive strength of concrete depends on the concrete composition, such as cement content and water–cement ratio. Therefore, L_t could be influenced by the cement and water–cement ratio used in the mix (Martí-Vargas *et al.*, 2012b). L_t also varies with advanced concrete properties developed to meet current construction practices, such as self-consolidating concrete, high-strength concrete and ultra-high performance concrete (Ramirez-Garcia *et al.*, 2016).

Geometry and surface condition of strands (d_s)

One key parameter that affects L_t is the available surface area of strands, which most codes take into consideration by using the stand diameter (d_s) as a parameter. Table 1 provides formulae for L_t in AASHTO LRFD (AASHTO, 2012), ACI 318 (ACI, 2014), Eurocode 2 (BSI, 2004), IRC 112 (IRC, 2012), fib-Model Code (fib-MC) (fib, 2010) and IS 1343 (BIS, 2012). These codes consider a linear relationship between L_t and d_s. However, many other factors (as discussed later) can also affect L_t, necessitating a more rational relationship with more influential factors. Another factor affecting L_t is the surface condition of the strands. A rough or indented strand surface helps in enhancing the friction between the strand and concrete, which in turn results in increased bonding and reduced L_t (Barnes *et al.*, 2003; Martin and Scott, 1976). During strand manufacture, the pre-treatment of strands, wire-drawing processes, use of lubricants (calcium salts of fatty acids,

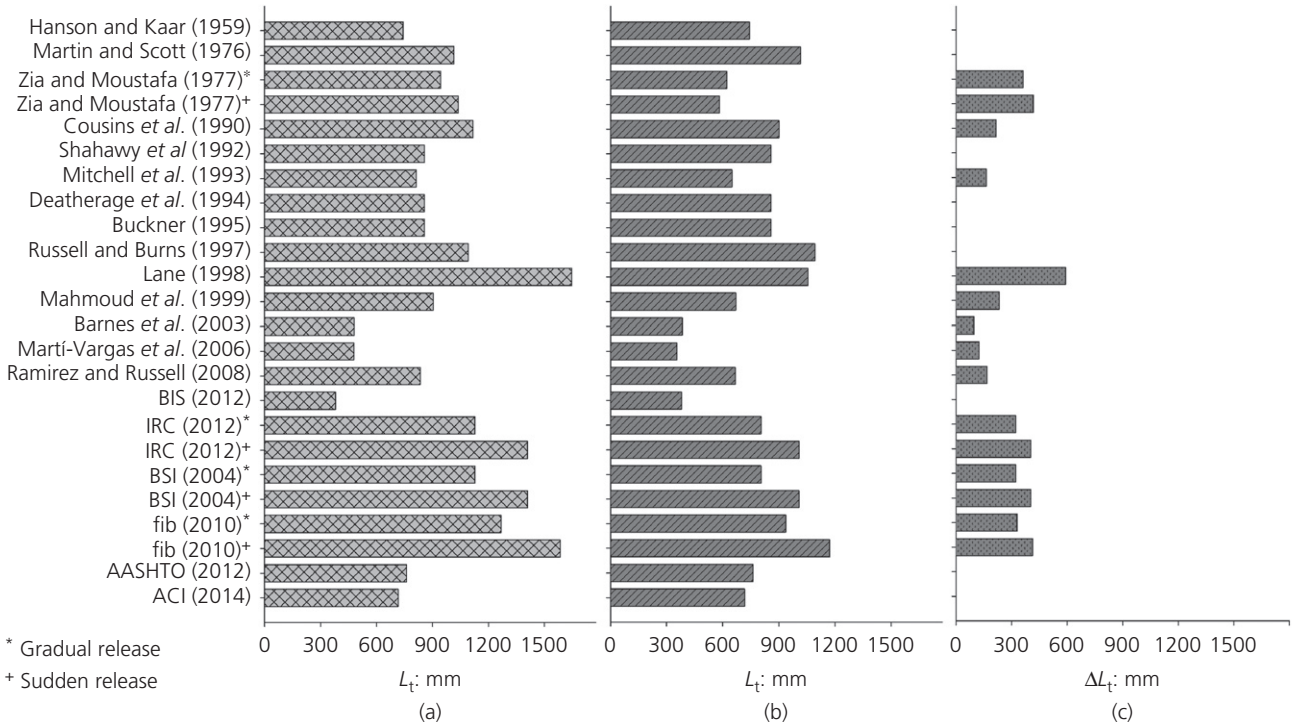

Figure 4. Design values of L_t based on codes and equations available in the literature (a) based on $f_{ci} = 23$ MPa; (b) based on $f_{ci} = 36$ MPa; (c) difference in L_t for (b) – (a)

Table 1. Formulae for L_t from standards

Code	Transmission length equation (SI units)
ACI 318 (ACI, 2014)	$L_t = \left(\frac{f_{pe}}{20{\cdot}7}\right) d_s$
AASHTO (2012)	$L_t = 60 d_s$
fib-MC (fib, 2010)	$L_t = \alpha_1 \alpha_2 \alpha_3 \frac{A_{ps}}{\pi d_s} \frac{f_{pi}}{\eta_{p1} \eta_{p2} f_{ctd}}$
Eurocode 2 (BSI, 2004) IRC 112 (IRC, 2012)	$L_t = \frac{\alpha_1 \alpha_2 d_s f_{pi}}{f_{bpt}}$
IS 1343 (BIS, 2012)	$L_t = 30 d_s$

sodium stearate, etc.) and cleaning process can alter the surface properties (Dang *et al.*, 2014; Rose and Russell, 1997). Moreover, the thickness of the residual lubricant film on the strand surface can vary from one manufacturer to the other. All these conditions could affect the S–C bond and L_t.

Influence of prestress releasing method

The prestress release method (e.g. sudden release or gradual release) can influence the dynamics of energy transfer from strand to concrete, and thereby influence L_t. In the case of sudden release, the PTC system does not get sufficient time to transfer the energy near the end portion of the strands – resulting in a longer L_t than for the case of gradual release (Barnes *et al.*, 2003; Rose and Russell, 1997). However, Russell and Burns (1997) indicated that the effect of the release method reduces as the length of the PTC element increases. Therefore, the gradual release method is recommended for laboratory studies on PTC specimens shorter than 3 m.

Time-dependent effects

The bond in PTC systems depends on the confinement provided by the concrete; it is activated as a consequence of radial interface displacement. The continued increase in the strength of concrete can enhance the S–C bond and could help in counteracting possible adverse effects due to long-term creep, shrinkage and relaxation (Barnes *et al.*, 2003; Bruce *et al.*, 1994; fib, 2000; Kaar *et al.*, 1963). Bruce *et al.* (1994) reported that seven-wire, 12·7 mm dia. strands embedded in concrete with $f_{ci} = 34$ MPa exhibited an increase in L_t by about 10 and 3% at 28 and 365 d, respectively. However, the same strand embedded in a weaker concrete ($f_{ci} = 27$ MPa) exhibited 20% increase in L_t in about 14 months, which is significant (Dorsten *et al.*, 1984). Caro *et al.* (2013) reported contradictory results on L_t with time. They observed that L_t either increased, decreased or did not change with time. Hence, time-dependent effects on L_t are important to understand and are discussed later in this paper.

Challenges in measuring strain in PTC systems

The transmission length of PTC specimens was determined based on the strain distribution along the length of the PTC members due to the prestress transfer. The strain on the strand or on the concrete surface along a line parallel to the strand can be measured to determine L_t. However, the placement of strain gauges on the helical outer wires of the seven-wire strand and the calculation of the corresponding axial strain in the strand are technically challenging. Also, pasting a number of gauges along the strand surface will affect the S–C bond. These factors could result in erroneous L_t measurement. Hence, researchers have developed a way to understand the strain in the strand indirectly from the strain on the concrete surface, which involves using a demountable mechanical strain gauge (DEMEC). It should be noted that the measurement of strain using a DEMEC gauge is highly sensitive to the pressure applied, the angle at which it is held, the posture and so on, leading to significant experimental or human error. If the concrete surface is good enough, this would give a reliable measurement of L_t, if several measurements are made across overlapping regions using a DEMEC and calculations are made by smoothing the data (Russell and Burns, 1997). This procedure (known as the ASM method and presented later) is used in this study.

Research significance

Significant number of pre-tensioned, HCSs without shear reinforcement or stirrups are being used in tall structures and industrial buildings. The shear resistance of HCS are highly dependent on the prestress transferred. Hence, the transmission length, L_t, is one of the important design parameters. This paper highlights the discrepancy existing among the design equations for L_t given in the literature and codes. If the design L_t is shorter than the actual L_t, it could lead to poor shear resistance of the HCS members. This paper finds that some codes underestimate L_t and provide less conservative shear designs. Based on experimental results, this paper proposes a new empirical equation to the IS 1343 and other codes to arrive at rational and conservative shear designs.

Current design provisions and differences

Table 1 provides various formulae published in the literature to determine L_t using various combinations of the influencing factors (AASHTO, 2012; ACI, 2014; BIS, 2012; BSI, 2004; fib, 2010; IRC, 2012). Figures 4(a) and 4(b) present L_t for a 12·7 mm dia., 1860 MPa grade, low-relaxation strand embedded in concrete with an f_{ci} of 23 and 36 MPa, respectively. Figure 4(c) shows the differences in L_t when the value of f_{ci} is increased from 23 to 36 MPa. In most cases, this difference is about 300 mm, which is significant. The L_t of the strand could be influenced by the area of contact between the strand and the concrete, the surface condition of the strand, stress in the steel and the prestress releasing method (Barnes *et al.*, 2003; Buckner, 1995; Cousins *et al.*, 1990; Deatherage *et al.*, 1994; Lane, 1998; Mahmoud *et al.*, 1999; Martí-Vargas *et al.*, 2006, 2007; Mitchell *et al.*, 1993; Ramirez-Garcia *et al.*, 2016; Shahawy *et al.*, 1992; Zia and Mostafa, 1977). These, and other factors influencing L_t, can be classified into two broad categories: (*i*) strand and associated properties and (*ii*) concrete and associated properties.

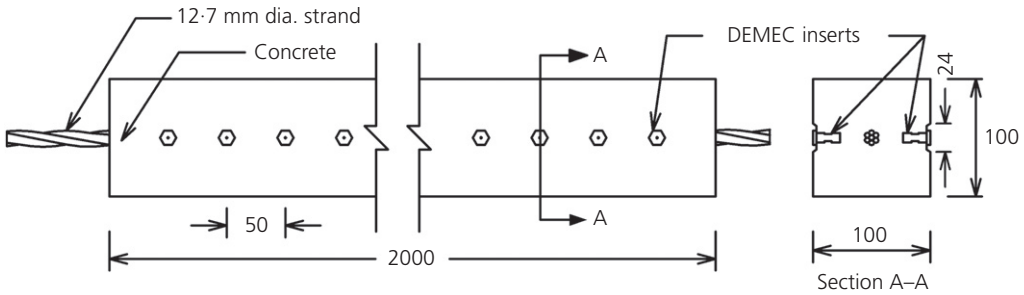

Figure 5. Transmission length specimen (dimensions in mm)

Strand and associated properties

The diameter (or contact surface) and surface condition of the strand can affect L_t. Although ACI 318 (ACI, 2014) states that many properties of the strand and concrete can influence L_t, it considers only f_{pe} and d_s to calculate L_t. Like ACI 318 (ACI, 2014), researchers have proposed equations for determining L_t by considering only f_{pi} and d_s (Buckner, 1995; Deatherage *et al.*, 1994; Shahawy *et al.*, 1992). As given in Table 1, AASHTO considers $L_t = 60d_s$, whereas IS 1343 (BIS, 2012) considers $L_t = 30d_s$, which is half of the value specified in AASHTO (2012). However, calculating L_t based only on d_s does not represent the actual L_t of the PTC system. According to Eurocode 2 (BSI, 2004), prestress is assumed to be transferred to the concrete by bond stress (f_{bpt}), which actually depends on both the steel and the concrete properties. The fib-MC (fib, 2010), Eurocode 2 (BSI, 2004) and IRC 112 (IRC, 2012) codes consider the tendon type, prestress releasing method and the bond condition to calculate L_t.

Concrete and associated properties

ACI 318 (ACI, 2014) does not consider f_{ci} to calculate L_t. The current formulation first appeared in ACI 318 (ACI, 1963), which was based on experimental work by Hanson and Kaar (1959) on PTC systems with concrete having a characteristic compressive strength of 20·7 MPa (3 ksi) (Tabatabai and Dickson, 1993; Zia and Mostafa, 1977). The value of L_t for today's concretes with higher-strength grades will be shorter than that for the PTC systems used by Hanson and Kaar (1959). Hence, the ACI 318 (ACI, 2014) equation could lead to overconservative designs. Similarly, AASHTO (2012) and IS 1343 (BIS, 2012) do not consider f_{ci} in calculating L_t. Eurocode 2 (BSI, 2004) considers f_{ci} to calculate the bond stress, which is used to calculate L_t. The National Cooperative Highway Research Program (NCHRP) report suggests an equation to determine the L_t by considering f_{ci} for high-strength concrete (Ramirez and Russell, 2008).

As shown in Figure 4(c), when f_{ci} increases from 23 to 36 MPa, L_t decreases by 29% (from 1128 to 805 mm). Similarly, fib-MC (fib, 2010) considers f_{ci} to determine the design tensile strength of concrete, which is then used to calculate L_t. Hence, L_t based on fib-MC (fib, 2010) decreased about 26% (from 1268 to 937 mm) when f_{ci} increased from 23 to 36 MPa. Conversely, the design L_t based on fib-MC (fib, 2010) is about 36% longer than that based on Eurocode 2 (BSI, 2004). Both Eurocode 2 (BSI, 2004) and fib-MC (fib, 2010) result in longer values of L_t than those based on AASHTO (2012), ACI 318 (ACI, 2014) or IS 1343 (BIS, 2012). Martí-Vargas and Hale (2013) found that the number of underestimated cases is less for Eurocode 2 than for US codes as they predict longer L_t. Many researchers have proposed empirical equations by accounting for f_{ci} (Barnes *et al.*, 2003; Cousins *et al.*, 1990; Lane, 1998; Mahmoud *et al.*, 1999; Martí-Vargas *et al.*, 2006, 2007; Mitchell *et al.*, 1993, Ramirez-Garcia *et al.*, 2016; Zia and Mostafa, 1977). The values of L_t calculated using these equations are also shown in Figures 4(a) and 4(b). Figure 4(c) shows that L_t could decrease by a maximum of 600 mm when f_{ci} increases from 23 to 36 MPa. Therefore, to determine L_t, f_{ci} is a crucial parameter to consider. However, there are very limited data on L_t for PTC systems with high-strength concretes. Such a database should be generated experimentally and incorporated into code formulations.

Experimental programme

Figure 5 shows a schematic diagram of the L_t test specimens with a 12·7 mm dia. strand embedded in a concrete prism (size: 100 × 100 × 2000 mm). Six specimens were prepared and tested. Three specimens each with concrete of f_{ci} equal to 23 and 36 MPa were prepared.

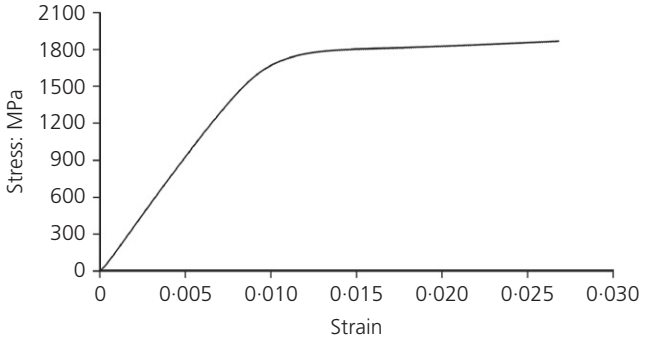

Figure 6. Stress–strain behaviour of seven-wire strand used

Table 2. Chemical composition of prestressed steel

Element	C	Si	Mn	P	Cr	Ni	Al	Co	Cu	S	Fe
Concentration: %	0·72	0·21	0·94	0·02	0·27	0·02	0·01	0·02	0·02	0·002	Remaining

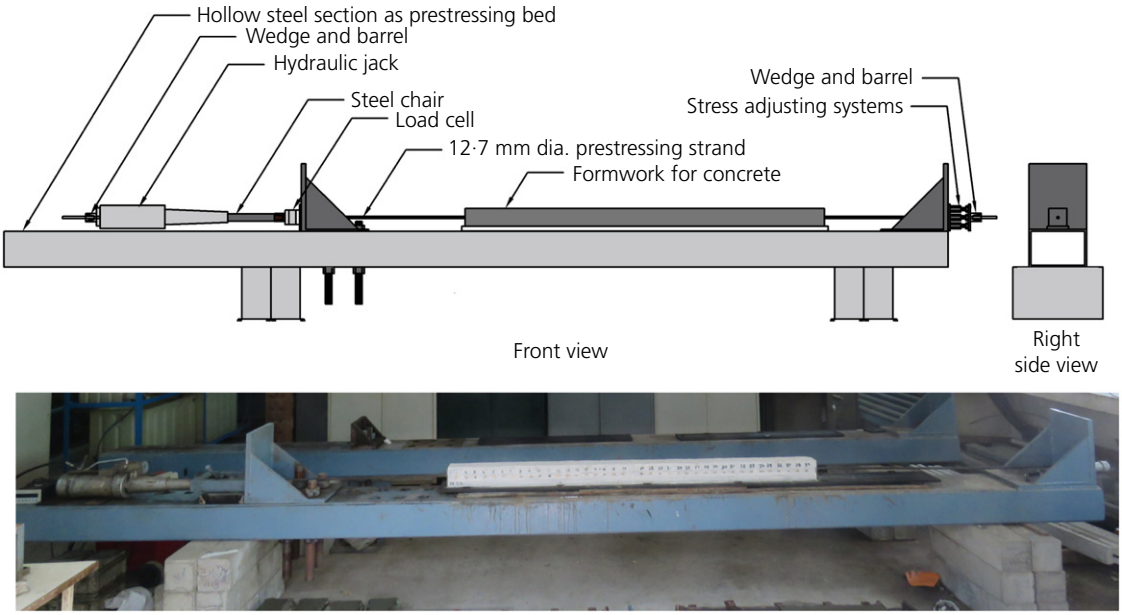

Figure 7. Prestressing bed and PTC specimen

Materials

The low-relaxation, seven-wire, prestressing strand with a diameter of 12·7 mm, a modulus of elasticity of ≈200 GPa, and an ultimate tensile strength of about 1860 MPa was used, meeting ASTM A 416 (ASTM, 2017), IS 1343 (BIS, 2012) and IS 14268 (BIS, 1995) specifications. The stress–strain behaviour of the seven-wire strand used is shown in Figure 6. Table 2 shows the chemical composition of the prestressing steel. A concrete with a slump of 100 ± 20 mm was used. OPC 53S grade finely ground cement was used to achieve early compressive strength gain to transfer the prestress. At the time of prestress transfer, the average cube-compressive strengths for two sets were 23 and 36 MPa, respectively. The average cube-compressive strengths of the concrete specimens at 28 d were 45 and 62 MPa, respectively. Hence, these concretes can be considered as M35 and M55 concretes.

Preparation of pretensioned concrete specimens

Figure 7 shows the prestressing bed and the PTC specimen. The self-equilibrating bench prestressing bed consisted of a hollow steel section and two end brackets. A 5·5 m long seven-wire strand was inserted in the through-holes of the end brackets. A hydraulic jack (300 kN capacity), steel chair and load cell (in this sequence) were placed at the live end to apply the stress, in order to activate the stress reaction and monitor the applied load. A hydraulic jack was used to apply the initial prestress of $0{\cdot}75f_{pu}$. A stress-adjusting system, wedges and barrel were placed at the dead end. A hexagonal nut and bolt arrangement was used as a stress-adjusting system, to transfer the prestress gradually from the strand to the hardened concrete. A polyvinyl chloride (PVC) mould was placed on the bed (around the strand) to cast the concrete prism. Prior to placing the concrete, hexagonal brass inserts or pins were affixed to the inside face of the PVC mould using acrylic strips (for accuracy in alignment). This alignment is crucial in obtaining good DEMEC data. Figure 8 shows the brass inserts in more detail. Concrete was prepared and placed in the PVC prism mould in one layer and compacted (25 tampings for every 100 mm of prism length). Six companion cube specimens were also prepared to determine f_{ci}. The L_t and cube specimens were moist cured (using wet sacking or plastic covers) until the concrete attained 60% of f_{ck} (e.g. about 3 d). Then, prestress was gradually transferred using the stress-adjusting system and L_t was measured. The average f_{pe} was about 1215 MPa.

Strain measurement and instrumentation

It was experimentally observed that the surface-mounted DEMEC discs were not suitable for long-term measurements. Hence, brass inserts or pins were used to obtain quality long-term data. These were custom-designed and fabricated as nut–bolt systems, using hexagonal brass rods (see Figure 8 for

details). These were spaced at 50 mm centre-to-centre along the centre line of the two opposite concrete surfaces, as shown in Figure 5. The distances between the brass inserts along the lengths of the specimens were measured before and after the transfer of prestress, and the strain along the concrete surface $\varepsilon_{c(x)}$ was determined. The DEMEC used in this study could measure over a distance of 150 ± 4 mm. Therefore, the DEMEC readings were taken with reference to a 150 mm gauge length and the strain $\varepsilon_{c(x)}$ was assigned to the midpoint of the gauge length, which is the distance between every $(n-1)$th to $(n+1)$th point (see Figure 9). Consequently, readings were taken for all the points on the concrete surface. The measured strain data were smoothed by averaging the strain data over the three consecutive and overlapping 150 mm gauge lengths. The smoothed strain at the xth point $\varepsilon'_{c(x)}$ was calculated as

$$1. \quad (\varepsilon'_c)_x = \frac{(\varepsilon_c)_{x-1} + (\varepsilon_c)_x + (\varepsilon_c)_{x+1}}{3}$$

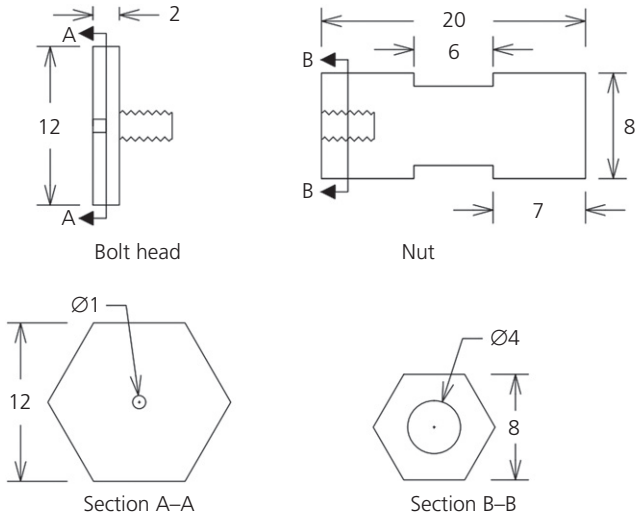

Figure 8. Custom-made DEMEC inserts (dimensions in mm)

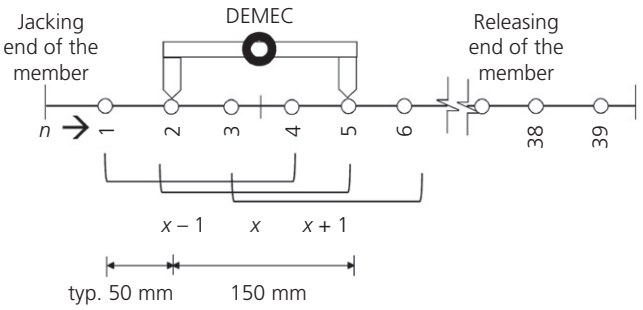

Figure 9. DEMEC reading on concrete surface

Table 3. Transmission length determined experimentally

f_{ci}: MPa	Specimen ID	$L_{t,measured}$: mm Jacking end	Releasing end	Average	$L_{t,avg}$: mm
23	f_{ci} 23-S1	630	565	597	582
	f_{ci} 23-S2	520	570	545	
	f_{ci} 23-S3	625	579	602	
36	f_{ci} 36-S1	480	498	489	463
	f_{ci} 36-S2	460	472	466	
	f_{ci} 36-S3	427	443	435	

As shown in Figure 2(b), the distance from the end of the specimen to the point where the strain becomes constant is L_t. However, such ideal cases were not observed in experiments. Hence, in this study, the value for 95% of the maximum average strain ($\varepsilon_{c,max}$) was calculated using the method (known as the ASM method) given by Russell and Burns (1997). This was used to determine the L_t of the PTC specimens.

Measured transmission length, $L_{t,measured}$

Influence of compressive strength of concrete

The values of L_t for all the specimens (denoted $L_{t,measured}$ herein) were experimentally obtained and compared with the value of L_t calculated using the equations in the codes (denoted as $L_{t,code}$ herein). Table 3 provides the values of $L_{t,measured}$ for the seven-wire strands embedded in two grades of concrete (Concretes A and B with f_{ci} of 23 and 36 MPa, respectively). Figures 10(a) and 10(b) show the strain profile of the concrete surface. The average of the maximum strains on the concrete surface, $\varepsilon_{c,max}$, for both Concretes A and B was about 524 microstrains. The average value of $L_{t,measured}$ was obtained as the distance from the end of the member to the point experiencing 95% of $\varepsilon_{c,max}$. These measurements were made on both the jacking and releasing ends – the left and right ends in Figure 10, respectively – and are provided in Table 3. Note that this test programme adopted the gradual stress releasing method and that the value of $L_{t,measured}$ is found to be similar at both the jacking and releasing ends – in agreement with Benítez and Galvez (2011). The average values of $L_{t,measured}$ of the seven-wire strand embedded in Concretes A and B were 463 and 582 mm, respectively, with coefficients of variation of about 5%, which is acceptable.

Figure 11 shows the values of $L_{t,measured}$ and $L_{t,code}$ obtained based on different codes. For both Concretes A and B, the values of $L_{t,measured}$ are shorter than the values of $L_{t,code}$ calculated using AASHTO (2012), ACI 318 (ACI, 2014), Eurocode 2 (BSI, 2004), IRC 112 (IRC, 2012) or fib-MC (fib, 2010). However, the value of $L_{t,measured}$ was significantly longer (by 22 and 53%, respectively) than the value of $L_{t,code}$ calculated using IS 1343 (BIS, 2012), leading to a possibly less conservative design. Note that the ACI, AASHTO and IS codes do not consider f_{ci} in calculating the $L_{t,code}$. From these results, when the average value of f_{ci} was increased from 23 to

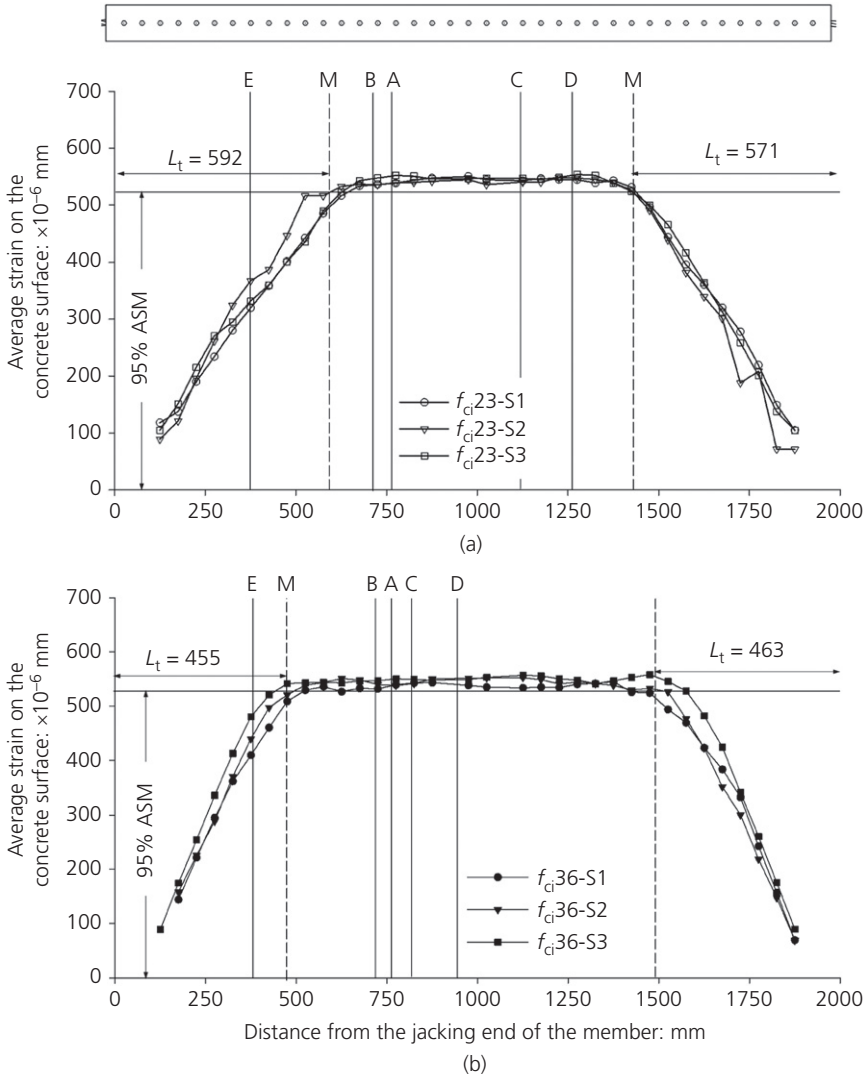

Figure 10. Values of $L_{t,measured}$ for: (a) $f_{ci} = 23$ MPa; (b) $f_{ci} = 36$ MPa. A, AASHTO LRFD (AASHTO, 2012); B, ACI 318 (ACI, 2014); C, Eurocode 2 (BSI, 2004) and IRC 112 (IRC, 2012); D, fib-MC (fib, 2010); F, IS 1343 (BIS, 2012); M, $L_{t,measured}$

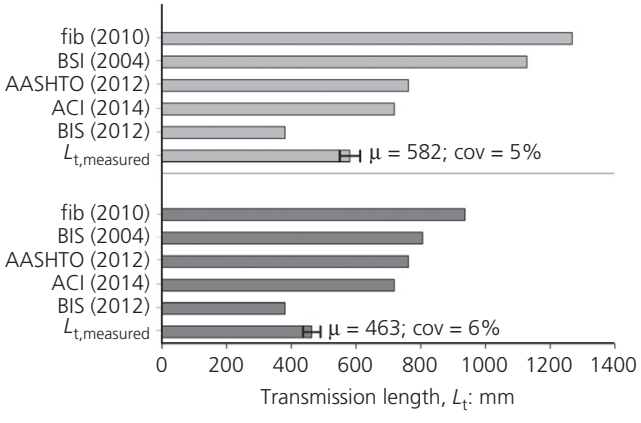

Figure 11. $L_{t,code}$ and $L_{t,measured}$: (a) Concrete A ($f_{ci} = 23$ MPa); (b) Concrete B ($f_{ci} = 36$ MPa). μ, mean; cov, covariance

36 MPa, the average value of $L_{t,measured}$ decreased by about 20%. The Eurocode 2 (BSI, 2004), IRC 112 (IRC, 2012) and fib-MC (fib, 2010) codes do consider f_{ci} in calculating $L_{t,code}$; hence, the values of $L_{t,code}$ reduced by 29 and 26%, respectively, when f_{ci} was increased from 23 to 36 MPa. For Concrete A, the ratios of $L_{t,code}$ to $L_{t,measured}$ based on the aforementioned AASHTO, ACI, IS, Eurocode 2, IRC and fib-MC codes were 1·31, 1·23, 0·65, 1·94 and 2·18, respectively. Similarly, these ratios for Concrete B were 1·65, 1·55, 0·82, 1·74 and 2·02, respectively. For the former three codes, the compressive strength is not considered; hence, these ratios increase as concrete strength increases. In the case of the latter two codes, the compressive strength is considered; hence, these ratios decrease as concrete strength increases, which is more realistic. This highlights the importance of using f_{ci} as an influencing parameter in the equations for $L_{t,code}$. Moreover,

when this ratio is greater than 1, the design would be conservative and vice versa. Therefore, the AASHTO, ACI, Eurocode 2, IRC and fib-MC codes provide conservative designs and the IS 1343 (BIS, 2012) provides a non-conservative design.

This study highlights the need for including the term f_{ci} in the equations for $L_{t,code}$. Based on the experimental results, for example, the equation given in ACI 314 (ACI, 2014) can be modified by incorporating f_{ci} and a correction factor for f_{ci}, α, as

$$2. \quad L_t = \left(\frac{1}{\alpha}\right)\left(\frac{f_{pe}}{f_{ci}}\right)d_s$$

Equation 2 was calibrated using the experimental data, and the values of α for f_{ci} equal to 23 and 36 MPa were estimated to be 1·11 and 0·94, respectively. Owing to the lack of extensive data on the effect of compressive strength, a linear relationship can be assumed and the correction factor, α, can be formulated as

$$3. \quad \alpha = 1{\cdot}41 - 0{\cdot}013 f_{ci}$$

This can be used for applications with other concrete grades in use. When additional data on $L_{t,measured}$ from strands embedded in concretes with other strength grades are available, Equation 3 can be modified.

Variation of $L_{t,measured}$ with time

Figure 12 shows the variation of strain (along the length of the specimen) as a function of exposure time for Concretes A and B. It also shows the average $L_{t,measured}$ of each specimen at 0 and 250 d after the stress transfer (denoted $L_{t,0}$ and $L_{t,250}$). Table 4 presents the detailed measurements made on the jacking and releasing ends and the average value of $L_{t,measured}$ for all the specimens with respect to time. The horizontal dashed lines indicate the 95% $\varepsilon_{c,max}$ at 0, 150, 200, and 250 d of exposure. At the time of stress transfer, the $\varepsilon_{c,max}$ for all the specimens was about 500 microstrains. By 250 d of exposure,

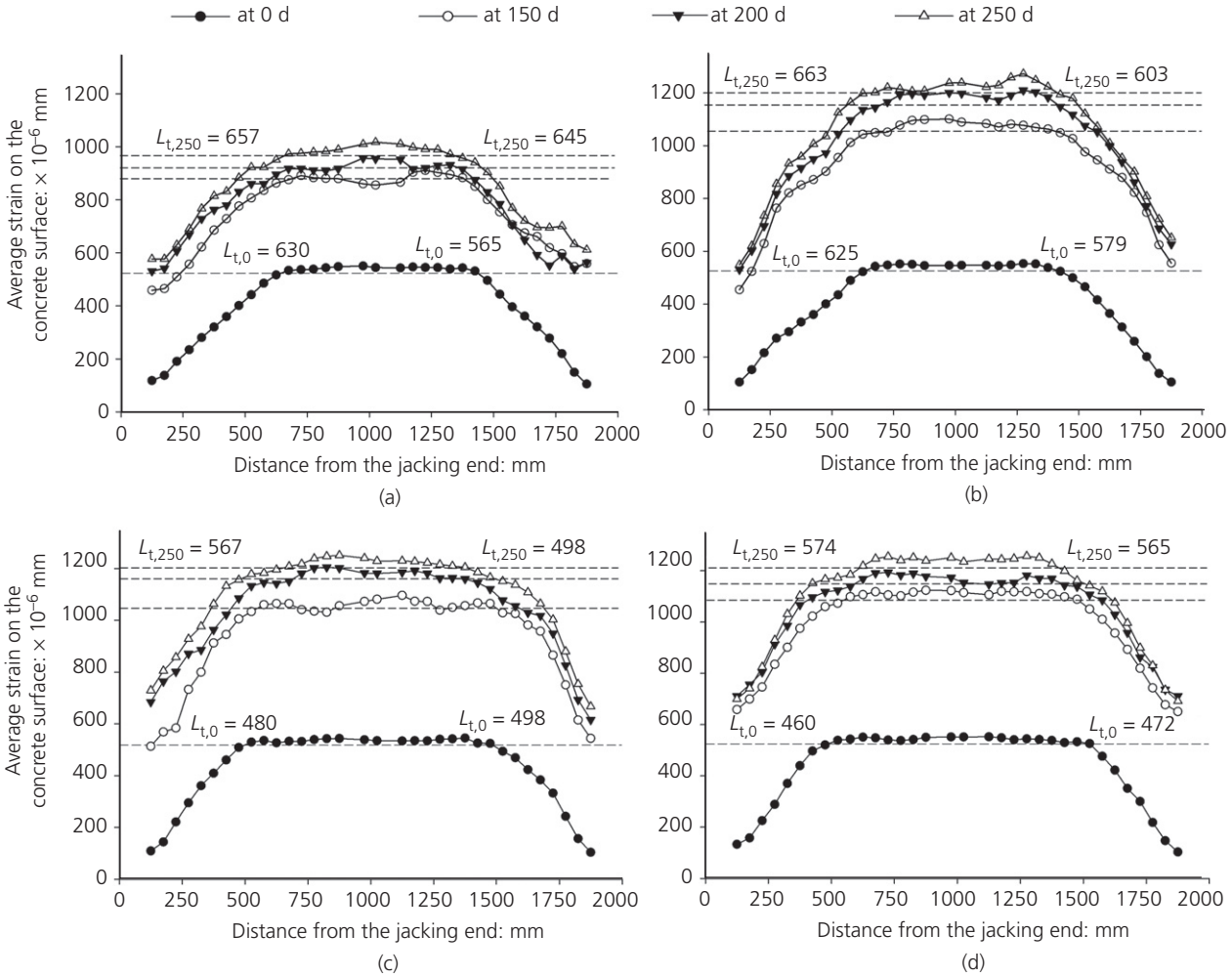

Figure 12. Time-dependent $L_{t,measured}$ for Concretes A and B: (a) f_{ci}, 23-S1; (b) f_{ci}, 23-S2; (c) f_{ci}, 36-S1; (d) f_{ci}, 36-S2

Table 4. Measured L_t variation as a function of time (in days)

	Transmission length, $L_{t,measured}$: mm												Change in L_t	
	$L_{t,0}$ (at transfer)			$L_{t,150}$			$L_{t,200}$			$L_{t,250}$				
Specimen ID	JE	RE	Avg	JE	RE	Avg	JE	RE	Avg	JE	RE	Avg	mm	%
f_{ci} 23-S1	630	565	597	640	619	630	648	620	634	657	645	651	54	9
f_{ci} 23-S2	625	579	602	631	578	605	663	580	622	663	603	633	31	4
f_{ci} 36-S1	480	498	489	529	501	515	559	564	562	567	560	564	75	15
f_{ci} 36-S2	460	472	466	506	497	502	538	522	530	574	565	570	64	22

JE, jacking end; RE, releasing end; Avg, average

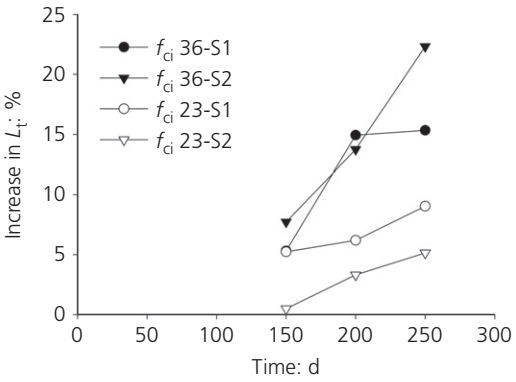

Figure 13. Increase in L_t with time for Concretes A and B

this increased to about 1100 and 1250 microstrains for Concretes A and B, respectively.

Figure 13 shows the increase in $L_{t,measured}$ as a function of time. At 150 d, the average of this increase can be about 5 and 7% for Concretes A and B, respectively. At 250 d, the value of L_t increased by an average of about 8 and 18% for Concretes A and B, respectively. Low-relaxation strands, meeting ASTM A 416 (ASTM, 2017) were used in this study. Hence, the observed change in L_t (by about 18%) could be mainly due to creep and shrinkage of concrete. Further testing on similar specimens is required to comment more on these numbers and the rate of change of L_t. In general, it can be concluded that the rate of change of L_t after 150 d is not significant.

Shear resistance of HCS – a case study

L_t of prestressed strands plays a crucial role in achieving the desired shear capacity ($V_{n,max}$) within the shear-critical region, especially when the elements do not have shear stirrups. To ease the placement of concrete (casting), it is common not to use stirrups in the pretensioned HCSs and rely on the prestressed strands to achieve the desired shear resistance.

Mechanistic and code equations for $V_{n,max}$

The shear force required to cause an inclined crack can be calculated as the shear force required to cause a principal tensile stress equal to the tensile strength of the concrete at the centroid of the beam. The nominal shear resistance of PTC systems is given in Equation 4 (Nawy, 2003).

Table 5. Equations provided in various codes and standards for web shear capacity

Code	Web shear capacity (SI units)
ACI 318 (ACI, 2014)	$V_{cw} = \left(0{\cdot}29\lambda\sqrt{f'_c} + 0{\cdot}3f_{cp}\right)b_w d$
fib-MC (fib, 2010)	$V_{cw} = \frac{0{\cdot}8Ib_w}{Q}\sqrt{f_{ctd}^2 + \alpha_1 f_{cp} f_{ctd}}$
Eurocode 2 (BSI, 2004)	$V_{cw} = \frac{Ib_w}{Q}\sqrt{f_{ctd}^2 + k_1 f_{cp} f_{ctd}}$
IS 1343 (BIS, 2012)	$V_{cw} = 0{\cdot}67 b_w d\sqrt{f_t^2 + 0{\cdot}8 f_{cp} f_t}$

4. $$V_n = V_c + V_s + V_p$$

where V_n is the nominal shear force and V_c, V_s and V_p are the shear capacity contributed by the concrete, steel stirrups and prestressed strands (vertical component only), respectively. For HCS systems without shear reinforcement and with horizontal strands, V_s and V_p can be considered to be equal to zero. To be conservative, V_c is taken as the lesser of V_{cw} and V_{ci} (the ultimate shear resistance of sections that are uncracked and cracked in flexure, respectively). HCS systems can be considered as simply supported systems; in such systems, V_{cw} is found to be less than V_{ci}, especially near the supports. Hence, V_c can be considered to be equal to V_{cw}. Based on the principles of classical mechanics and Mohr's circle, V_{cw} is given as (Nawy, 2003)

5. $$V_c = V_{cw} = \frac{Ib_w}{Q}\sqrt{f_t^2 + f_{cp} f_t}$$

Table 5 presents the various code equations for calculating V_{cw}. Note that, to achieve a conservative design, ACI 318 (ACI, 2014), Eurocode 2 (BSI, 2004), fib-MC (fib, 2010) and IS 1343 (BIS, 2012) consider different resistance factors for the parameters in Equation 5.

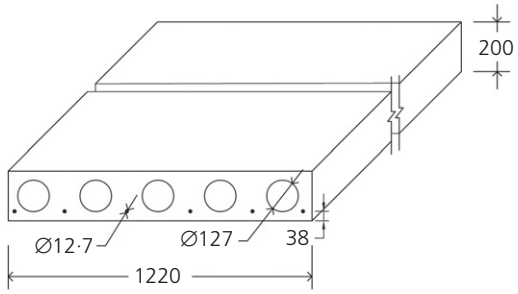

Figure 14. Cross-section of HCS used in this study (dimensions in mm)

Comparison between $L_{t,measured}$ and $L_{t,code}$

The shear design can be conservative if the value of $L_{t,measured}$ is adequate. However, if the value of $L_{t,measured}$ is inadequate, the available prestress at the shear-critical region would be less to resist the shear stresses. To understand the effect of L_t on the shear resistance of HCS members, a case study on the influence of L_t on the distance from the end of the member to the point where $V_{n,max}$ is achieved was performed. For this case study, a typical HCS design given in PCI (1999) was considered. As shown in Figure 14, the depth and width of this HCS were 200 and 1220 mm, respectively. There were six strands at 38 mm from the bottom of the slab. The value of $L_{t,code}$ calculated using the material properties and prestress levels in the current experiments and the ACI, Eurocode, fib, and IS codes were compared with the $L_{t,measured}$ obtained from the experiments.

For the selected HCS, the nominal shear resistance (denoted V_n) determined using values of $L_{t,measured}$ and $L_{t,code}$ calculated using the fib, ACI and IS codes are shown in Figure 15. Figure 15(a) indicates that fib-MC (fib, 2010) estimates $V_{n,max}$ of the HCS as 69 and 82 kN for Concretes A and B, respectively. As shown in Figure 15(b), ACI 314 (ACI, 2014) estimates $V_{n,max}$ of the HCS as 151 and 173 kN using Concretes A and B, respectively, which are almost twice the estimates of fib-MC (fib, 2010). As shown in Figure 15(c), IS 1343 (BIS, 2012) estimates intermediate values, of 118 and 137 kN. Based on $L_{t,measured}$ for Concretes A and B, the distances (from the end of the member) to achieve $V_{n,max}$ were about 0·6 and 0·5 m,

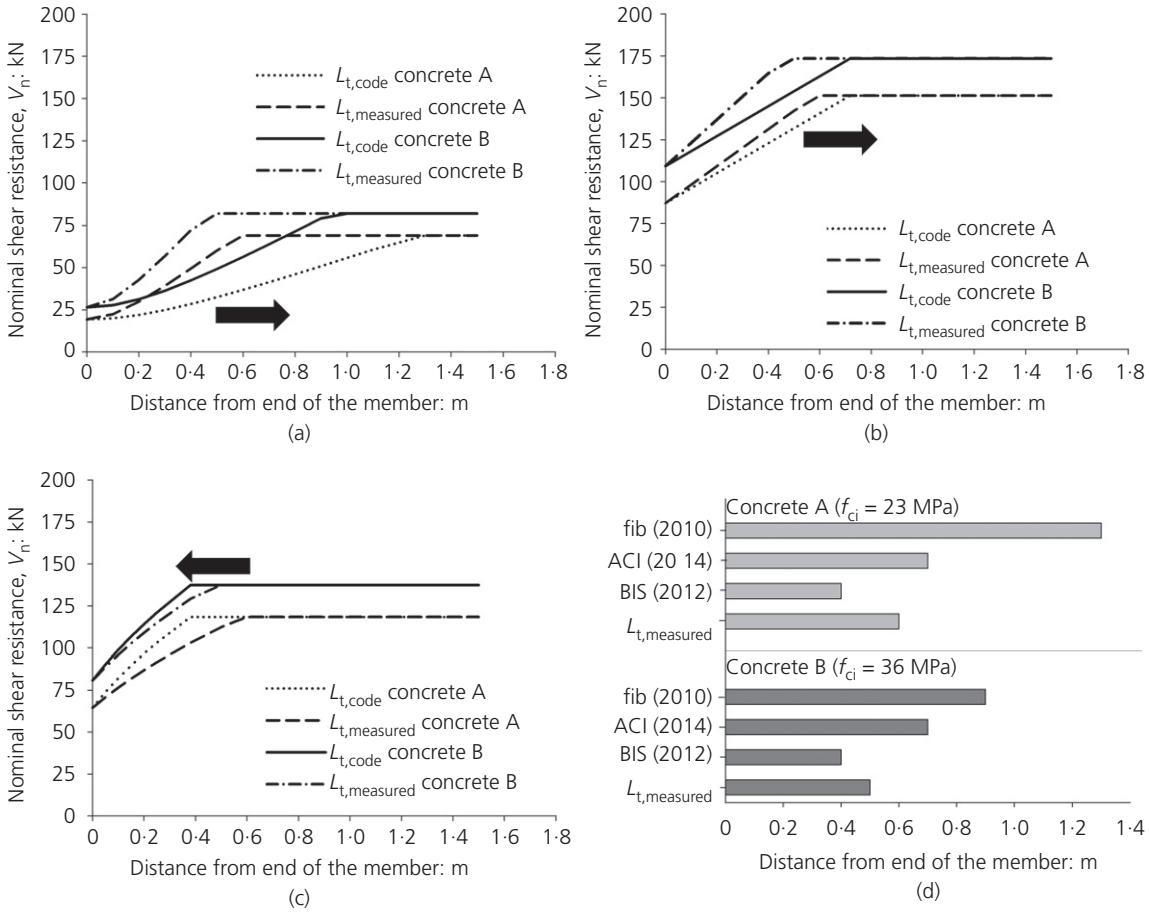

Figure 15. Shear resistance determined using different codes: (a) fib-MC (fib, 2010); (b) ACI 318 (ACI, 2014); (c) IS 1343 (BIS, 2012). (d) Distance to reach $V_{n,max}$

respectively, whereas, for both Concretes A and B, ACI 318 (ACI, 2014) estimated this distance as about 0·7 m and IS 1343 (BIS, 2012) estimated this distance as about 0·4 m. There is no difference for Concretes A and B because the ACI and IS equations do not consider f_{ci} in calculating $L_{t,code}$. The fib-MC code (fib, 2010) estimated a distance of 0·9 m to achieve $V_{n,max}$ for Concrete B, with $f_{ci} = 36$ MPa. For Concrete A, with $f_{ci} = 23$ MPa, this is about 1·3 m, which is 44% longer than the estimate for Concrete B. Using equations that incorporate f_{pe} or f_{ci}, or both, will ensure that sufficiently long estimates of L_t are used for design purposes and sufficient shear resistance is achieved within the shear-critical regions – as adopted by fib-MC and ACI (but not by IS).

As mentioned earlier, IS 1343 (BIS, 2012) estimates L_t as 30 (d_s), which leads to a condition where $V_{n,max}$ is achieved at a shorter distance than $L_{t,measured}$. For Concretes A and B, these were 0·2 and 0·1 m, respectively, shorter than $L_{t,measured}$. This could lead to a less conservative design. Therefore, it is proposed that IS 1343 (BIS, 2012) uses Equations 2 and 3 with f_{pe}, d_s, f_{ci} and α to estimate $L_{t,code}$ and arrive at conservative shear designs. Such sophisticated design approaches become very important, especially when quality control measures at the site are not stringent enough.

Summary and conclusions

The transmission length, L_t, for PTC systems with $f_{ci} = 23$ and 36 MPa strength concretes were estimated using the existing equations in the literature and codes. These estimates were compared with experimentally obtained values of L_t (denoted $L_{t,measured}$) of six prismatic PTC specimens made using 12·7 mm dia. strand and $f_{ci} = 23$ and 36 MPa strength concretes. A case study was performed to understand the influence of L_t on the shear resistance of pretensioned HCS. Based on this study, the following conclusions are drawn. From this study, it is evident that f_{ci} is one of the important parameters that can affect the L_t of PTC systems. The $L_{t,measured}$ significantly decreased by about 20% when f_{ci} increased from 23 to 36 MPa. It was observed that the $L_{t,code}$ based on AASHTO, ACI, Eurocode/IRC and fib-MC codes are longer than $L_{t,measured}$ for both $f_{ci} = 23$ and 36 MPa. From the case study, it was found that ACI 318 (ACI, 2014) and fib-MC (fib, 2010) provide sufficiently long estimates of L_t by considering more parameters defining the bond stress (i.e. f_{pe}, d_s, f_{ci}, etc.) than just the diameter of strand, d_s. Such an approach could lead to a conservative shear design by overestimating the required L_t in the end zone. However, L_t based on IS 1343 (BIS, 2012) is less than the $L_{t,measured}$ for both $f_{ci} = 23$ and 36 MPa, indicating a less-conservative shear design. Hence, based on the experimental study, this paper proposes an equation to calculate the L_t as follows.

$$6. \quad L_t = [(f_{pe} \times d_s)/(\alpha \times f_{ci})]$$

where the f_{ci} correction factor $\alpha = (1{\cdot}4 - 0{\cdot}013\, f_{ci})$.

Acknowledgements

The authors acknowledge financial support from the Fund for Improvement of Science & Technology Infrastructure, the Department of Science and Technology, and the Ministry of Human Resource Development, of the Government of India through the Department of Civil Engineering, Indian Institute of Technology Madras, Chennai. The authors also acknowledge assistance from the laboratory staff and students in the Construction Materials Research Laboratory at the Indian Institute of Technology Madras.

REFERENCES

AASHTO (American Association of State Highway and Transportation) (2012) *LFRD Bridge Design Specifications*, 6th edn. AASHTO, Washington, DC, USA.

ACI (American Concrete Institute) (1963) ACI 314-1963: Building code requirements for structural concrete and commentary. ACI, Detroit, MI, USA.

ACI (2014) ACI 314-2014: Building code requirements for structural concrete and commentary. ACI, Detroit, MI, USA.

ASTM (2017) A 416: Standard specification for low-relaxation, seven-wire steel strand for prestressed concrete. ASTM International, West Conshohocken, PA, USA.

Barnes RW, Grove JW and Burns NH (2003) Experimental assessment of factors affecting transfer length. *ACI Structural Journal* **100(6)**: 740–748.

Benítez JM and Gálvez JC (2011) Bond modelling of prestressed concrete during the prestressing force release. *Materials and Structures* **44(1)**: 263–278.

BIS (Bureau of Indian Standards) (1995) IS 14268: Uncoated stress relieved low relaxation seven-ply strand for prestressed concrete – specification. Bureau of Indian Standards, New Delhi, India.

BIS (2012) IS 1343: Prestressed concrete – code of practice. Bureau of Indian Standards, New Delhi, India.

Bruce RN, Russell HG, Roller JJ and Martin BT (1994) *Feasibility Evaluation of Utilizing High-Strength Concrete in Design and Construction of Highway Bridge Structures*. Louisiana Transportation Research Center, Baton Rouge, LA, USA, Report no. FHWA/LA-94-282.

BSI (2004) BS EN 1992-1-2:2004: Eurocode 2: Design of concrete structures – part 1-2: general rules for buildings. BSI, London, UK.

Buckner CD (1995) A review of strand development length for pretensioned concrete members. *PCI Journal* **40(2)**: 84–105.

Caro LA, Martí-Vargas JR and Serna P (2013) Time-dependent evaluation of strand transfer length in pretensioned prestressed concrete members. *Mechanics of Time-Dependent Materials* **17(4)**: 501–527.

Cousins TE, Johnston DW and Zia P (1990) Transfer length of epoxy-coated prestressing strand. *ACI Materials Journal* **87(3)**: 193–203.

Dang CN, Murray CD, Floyd RW and Hale WM (2014) Analysis of bond stress distribution for prestressing strand by standard test for strand bond. *Engineering Structures* **72**: 152–159.

Deatherage JH, Burdette EG and Chew CK (1994) Development length and lateral spacing requirements of prestressing strand for prestressed concrete bridge girders. *PCI Journal* **39(1)**: 70–83.

Dorsten V, Hunt FF and Preston HK (1984) Epoxy coated seven-wire strand for prestressed concrete. *PCI Journal* **29(4)**: 100–109.

Elliott KS (2014) Transmission length and shear capacity in prestressed concrete hollow core slabs. *Magazine of Concrete Research* **66(12)**: 585–602.

fib (International Federation for Structural Concrete) (2000) *Bond of Reinforcement in Concrete State of the Art Report*. fib, Lausanne, Switzerland, fib Bulletin No. 10.

fib (2010) *Model Code for Concrete Structures*. fib, Lausanne, Switzerland, fib Bulletin No. 55.

Hanson NW and Kaar PH (1959) Flexural bond tests of pretensioned prestressed beams. *Journal of the American Concrete Institute* **55(51)**: 783–802.

Hoyer E and Friedrich E (1939) Beitrag zur frage der haftspannung in eisenbetonbauteilen. *Beton und Eisen* **50(9)**: 717–736. (in German).

IRC (Indian Roads Congress) (2012) IRC 112: Code of practice for concrete road bridges. IRC, New Delhi, India.

Janney JR (1954) Nature of bond in pre-tensioned prestressed concrete. *Journal of the American Concrete Institute* **25(9)**: 717–736.

Kaar PH, Lafraugh RW and Mass MA (1963) Influence of concrete strength on strand transfer length. *PCI Journal* **8(5)**: 47–67.

Lane S (1998) *A New Development Length Equation for Pretensioned Strands in Bridge Beams and Piles. FHWA-RD-98-116*. Federal Highway Administration, Mclean, VA, USA.

Mahmoud ZI, Rizkalla SH and Zaghloul EER (1999) Transfer and development lengths of carbon fiber reinforced polymers prestressing reinforcement. *ACI Structural Journal* **96(4)**: 594–602.

Martin BLD and Scott NL (1976) Development of prestressing strand in pretensioned members. *Proceedings of ACI Journal* **73(8)**: 453–456.

Martí-Vargas JR and Hale WM (2013) Predicting strand transfer length in pretensioned concrete: Eurocode versus North American practice. *Journal of Bridge Engineering* **18(12)**: 1270–1280.

Martí-Vargas JR, Serna-Ros P, Fernandez Prada MA and Miguel Sosa PF (2006) Test method for determination of the transmission and anchorage lengths in prestressed reinforcement. *Magazine of Concrete Research* **58(1)**: 21–29.

Martí-Vargas JR, Arbelaez CA, Serna-Ros P, Navarro-Gregori J and Pallarés-Rubio L (2007) Analytical model for transfer length prediction of 13 mm prestressing strand. *Structural Engineering and Mechanics* **26(2)**: 211–229.

Martí-Vargas JR, Serna-Ros P, Navarro-Gregori J and Pallarés L (2012a) Bond of 13 mm prestressing steel strands in pretensioned concrete members. *Engineering Structures* **41**: 403–412.

Martí-Vargas JR, Serna P, Navarro-Gregori J and Bonet JL (2012b) Effects of concrete composition on transmission length of prestressing strands. *Construction and Building Materials* **27(1)**: 350–356.

Mitchell D, Cook WD and Khan AA (1993) Influence of high strength concrete on transfer and development length of pretensioning strand. *PCI Journal* **38(3)**: 52–66.

Nawy EG (2003) *Prestressed Concrete: A Fundamental Approach*, 4th edn. Pearson Eduction, Upper Saddle River, NJ, USA.

Oh BH and Kim ES (2000) Realistic evaluation of transfer lengths in pretensioned, prestressed concrete members. *ACI Structural Journal* **97(6)**: 821–830.

PCI (Precast/Prestressed Concrete Institute) (1999) *PCI Design Handbook: Precast and Prestressed Concrete*, 5th edn. Precast/Prestressed Concrete Institute, Chicago, IL, USA.

Ramirez J and Russell B (2008) *Transfer, Development, and Splice Length for Strand/Reinforcement in High-Strength Concrete. NCHRP Report 603*. Transportation Research Board, Washington, DC, USA.

Ramirez-Garcia AT, Floyd RW, Hale WM and Martí-Vargas JR (2016) Effect of concrete compressive strength on transfer length. *Structures* **5**: 131–140.

Rose DR and Russell BW (1997) Investigation of standardized tests to measure the bond performance. *PCI Journal* **44(4)**: 56–80.

Russell BW and Burns NH (1997) Measurement of transfer lengths on pretensioned concrete elements. *Journal of Structural Engineering* **123(5)**: 541–549.

Shahawy MA, Issa M and Batchelor B (1992) Strand transfer lengths in full scale AASHTO prestressed concrete girders. *PCI Journal* **37(3)**: 84–86.

Tabatabai H and Dickson T (1993) The history of the prestressing strand development length equation. *PCI Journal* **38(6)**: 64–75.

Zia P and Mostafa T (1977) Development length of prestressing strands. *PCI Journal* **22(5)**: 54–65.

How can you contribute?

To discuss this paper, please submit up to 500 words to the editor at journals@ice.org.uk. Your contribution will be forwarded to the author(s) for a reply and, if considered appropriate by the editorial board, it will be published as a discussion in a future issue of the journal.